MOLECULAR FRONTIERS JOURNAL

Inhaled Water and Salt Suppress Respiratory Droplet Generation and COVID-19 Incidence and Death on US Coastlines

Rachel D. Field[1], Nathan Moelis[2], Jonathan Salzman[3], Adriaan Bax[4], Dennis Ausiello[5], Sophie M. Woodward[6], Xiao Wu[6], Francesca Dominici[6] and David A. Edwards[7,3*]

Dry air alters salt and water balance in the upper airways and increases the risks of COVID-19 among other respiratory diseases. We explored whether such upper airway variations in salt and water balance might alter respiratory droplet generation and potentially contribute to observed impacts of airway hydration on respiratory disease. In a randomized 4-arm study of 21 healthy human subjects we found that the breathing of humid air, the wearing of cotton masks, and the delivery of (sodium, calcium, and magnesium chloride) salt droplets sized to deposit in the nose, trachea, and main bronchi similarly reduce the exhalation of respiratory droplets by approximately 50% ($P < 0.05$) within 10 minutes following hydration. Respiratory droplet generation returns to relatively high baseline levels within 60–90 minutes on return to dry air in all cases other than on exposure to divalent (calcium and magnesium) salts, where suppression continues for 4–5 hours. We also found via a preliminary ecological regression analysis of COVID-19 cases in the United States between January 2020 and March 2021 that exposure to elevated airborne salt on (Gulf and Pacific) US coastlines appears to suppress by approximately 25%–30% ($P < 0.05$) COVID-19 incidence and deaths per capita relative to inland counties — accounting for ten potential confounding environmental, physiological, and behavioral variables including humidity. We conclude that the hydration of the upper airways by exposure to humidity, the wearing of masks, or the breathing of airborne salts that deposit in the upper airways diminish respiratory droplet generation and may reduce the risks of COVID-19 incidence and symptoms.

Keywords: COVID-19; Aerosols; Humidity; Salt; Calcium; Ecological Regression; Respiratory Disease; Respiratory Droplets.

INTRODUCTION

When we breathe, air — hot or cold, moist or dry, dirty or clean — enters the nose and mouth and quickly enters the trachea and main bronchi. Incoming air then slows down, mixing with air that is saturated with moisture[1], gases that reflect our phenotypical state[2], and airborne particles that are an expression of the air we breathe and the fragility of our airway lining mucus[3]. In this zone of the nasopharynx and upper airways, most of the particles we breathe fall out of the air and onto a mucus layer[4]. The air itself is meanwhile heated or cooled to 37°C, while beyond the carina air humidity climbs to 100% — the microclimate conditions of the lungs[1]. The hydration of the nasopharynx and upper airways evolves by the way of this vital heat and mass exchange with incoming

[1]School of Engineering & Applied Sciences, Columbia University, NY, NY. [2]School of Bioengineering, Northeastern University, Huntington Avenue [3]Sensory Cloud, 650 East Kendall St, Cambridge, MA. [4]National Institutes of Health, Bethesda, MD. [5]Massachusetts General Hospital & Harvard Medical School, Boston, MA. [6]Harvard T.H. Chan School of Public Health, Boston, MA. [7]John A Paulson School of Engineering & Applied Sciences, Harvard University, Cambridge, MA. *Correspondence should be addressed to: David Edwards, dedwards@seas.harvard.edu, 118 Pierce Hall, Harvard University, Cambridge MA 02138. Published online 31 August 2021; doi:10.1142/S2529732521400058

air, as do the biophysical properties of the mucus that lines the nose and upper airways.

The hydration of the upper airways influences the ability of airway lining mucus to clear the hundreds of millions to tens of billions of particles that fall onto it every day — and this matters to respiratory health in ways that continue to be actively explored[5]. The clearance of inhaled and deposited allergens, pathogens, and other contaminants is essential for the avoidance of respiratory disease, which, with the worsening of air pollution, now counts as the leading cause of death in low-income countries of the world[6].

The dehydration of the upper airways by the breathing of any air that is not saturated at 37°C elevates the concentration of natural salts and other osmotic constituents of airway lining fluid, helping maintain proper hydration on the breathing of moderately humid air[7]. The osmotic-mediated hydration of the upper airways, a phenomenon as inevitable as oxygen absorption by the peripheral lung (rarely do we breathe air so saturated as the air within our lungs), facilitates the natural ability of mucus to clear deposited particles by the way of cilia motion toward the mouth[8].

On the sustained breathing of very dry air, the thinning of airway lining fluid leads to increased mucus secretion[9], cilia loss, and inflammation, and slower cilia beat frequency[10]. These and other upper airway mucosal and peripheral lung immunological consequences of the breathing of dry air heighten the risk of chronic lung diseases, such as asthma[11] and COPD[12], and airborne infectious diseases, such as influenza[13] and COVID-19[14]. While the breathing of properly humidified air reestablishes the normal osmotic-mediated hydration of the upper airways, the inhalation of airborne salts is the more effective natural pathway for the hydration of the upper airways[7]. Salts in the atmosphere originate most commonly in sea-spray aerosols (SSA), generated by the action of wind over the ocean surface, with most significant airborne salt concentrations at or above wind speeds of approximately 2 m/s[15]. Sea salts, physiologically natural chloride salts of sodium, magnesium, calcium, and potassium, are abundant in the air up to 40 m over the ocean surface, and within typically approximately half a kilometer of sea coasts[16], while submicron salt particles exist throughout the earth's atmosphere[17]. Inhaling these salts as dry particles or in droplets at hypertonic concentrations promotes the osmotic hydration of the airways[18], increasing cilia beat frequency. The cessation of exposure to airborne salt, whether post environmental exposure or following aerosol delivery, leads to a cessation of the cilia beat frequency benefit within approximately 30 minutes[19], and actually poorer upper airway clearance over longer times[20]. Physiological salts are delivered to the airways in the treatment of cystic fibrosis[21] for mucus cleansing and decongestion in the form of nasal saline sprays and gavages[22] and for overall respiratory health by speleotherapy — the breathing of air in salt mines, a practice dating from 19th century European observations that salt mine workers suffered less respiratory disease than everyone else[23] — and the contemporary practice of halotherapy[24].

The impact of breathing on the upper airways is highly conditioned by the formation of the "laryngeal jet"[25] of air that forms within the trachea and can reach near turbulent air speeds at the moment of peak inspiratory air flow[25]. Incoming air can destabilize mucus surfaces in the trachea and main bronchi, forming tiny droplets of mucus as wind on the sea generates sea spray[26]. The propensity of mucus to disintegrate into respiratory droplets is inversely (if weakly) proportional to the surface tension of mucus[27] and strongly proportional to the surface elasticity of mucus[28], the latter representing the ease with which the mucus surface can be stretched. Under the shear force of incoming and outgoing air, highly elastic mucus surfaces, characterized by a mixture of surface-active substances ranging from lung surfactants and mucins to inhaled hydrophobic particles, tend to form waves and subsequently to break up into droplets[29]. In vitro experiments that impose a "laryngeal jet" force of air on mucus and mucus mimetic surfaces[27,28] have shown that mucus surfaces break up into small droplets in proportion to surface elasticity[30], and that this elasticity is reduced by monovalent (sodium) and divalent (calcium) chloride salts[31], while it can be increased by the topical delivery of surfactants[27,28]. These same effects have been demonstrated during normal human breathing in the case of sodium chloride[32] and calcium chloride salt inhalation[33,34] (where respiratory droplet generation is suppressed) and in the case of lung surfactant inhalation[32] (where respiratory droplet generation is increased). Increases and decreases in mucus droplet generation impact upper airway mucus clearance function, since respiratory droplets can shuttle foreign contaminants from upper airway mucus to the lower respiratory tract and back into the environment — a recognized mode of airborne respiratory disease transmission[35] and a particular facilitator of the COVID-19 pandemic[36].

This study examines exhaled aerosol in healthy human subjects in several protocols that altered the humidity and salinity of the inhaled air, and preliminarily the association between county-level COVID-19 incidence and death rate with proximity to seacoasts where airborne salt levels are particularly high.

METHODS

Study design and participants

Twenty-one healthy human subjects, ages 18–66, body mass index (BMI) 19–33, were randomly assigned to one or more protocols that exposed them to air with varying amounts and compositions of water and salt in vapor and droplet forms. We hypothesized that one of the consequences of hydration

and dehydration of the upper airways might be to modulate respiratory droplet generation itself. Varying volumes of water in the upper airways promote not only varying salt concentrations but varying surfactant concentrations, as well — and these might alter surface properties of airway lining mucus, promoting or diminishing respiratory droplet generation. We measured exhaled aerosol in healthy human subjects in several protocols that altered the humidity and salinity of the inhaled air. We explored the effect of hydration on exhaled respiratory droplets via direct changes in the moisture of inhaled air, and, indirectly, via the wearing of cotton face masks, which have been observed to increase the moisture of inhaled air[37]. To investigate the osmotic regulation of respiratory droplet generation in the upper airways, we examined exhaled aerosol following the delivery of distilled water, isotonic saline, and hypertonic saline to the nose, trachea, and main bronchi with 9–10-μm-diameter droplets. All participants in the nasal inhalation studies were blinded to the composition of the water droplets inhaled. Given the known action of divalent calcium as chelator of anionic surfactants and sub-surface layer mucin proteins[27,28,31], we replaced sodium chloride in the inhaled droplets with calcium chloride (and magnesium chloride) to examine the importance of cationic-altered mucus surface properties in the prolongation of respiratory droplet regulation. To confirm calcium-specific effects related to the divalent nature of calcium, we repeated these studies replacing calcium with magnesium.

Procedures

Exhaled particles were measured before and after exposure to the varying amounts of airborne water and salt by a particle detector (Climet 450-t) designed to count airborne particles in the size range of 0.3 μm to greater than 5 μm. The particle detector air port was attached by a flexible plastic tube to the side (by a T connector) of a 1" inner diameter tube into which subjects inhaled and exhaled. The 1" tube connected at one end a mouthpiece provided with standard nebulizer tubing and at the other end a portable HEPA filter. The entire tubing system facilitated the filtration of all environmental particles from the lungs of subjects over a period of about 1 minute of breathing with subjects' lips tightly sealed around the mouthpiece and pinching their noses. The rate of flow of the particle counter (50 L/min) was near the typical peak inspiratory/expiratory rate of flow of human subject breathing such that the direction of air flow remained into the particle counter. Each standard nebulizer tubing and mouthpiece were removed from sealed packaging before each subject prior to the subject's first exhaled particle detection. On subsequent counting maneuvers the same mouthpiece, tubing and HEPA filter were reattached by the participant to insure the absence of contamination from one subject to the next. Before each test, the mouthpiece was replaced by a stopper and the particle detector was turned on to verify the absence of leakage of particles from the environment. Background of less than 10 particles per liter of air was deemed "well sealed." With the mouthpiece placed back onto the tubing, subjects performed normal tidal breathing through the mouthpiece while plugging their noses with their fingers over 1–2 minutes — beginning with two deep breaths to empty their lungs of environmental particles. Over this time frame, particle counts per liter of air pulled from the exhaled breath into the particle counter diminished and subsequently fluctuated around a baseline number. Given the assurance of no leakage from the outside environment, the tight lip seal, and the pinched nose, we assumed this baseline number to equate to the particles generated within the subject's airways. Once the lower plateau of particle counts was reached, subjects continued to breathe normally for the determination of exhaled aerosol particle number. Participants sat opposite to the study administrator with a plexiglass barrier in between. A second method for measuring exhaled particles, as described in the Supplemental Material, was used to benchmark the Climet method.

We maintained low humidity (10% relative humidity (RH)) by conducting our studies in an air-conditioned office in the winter season in Massachusetts. We elevated humidity in a second office by means of a humidifier (Vornado Ultra3 Whole Room Ultrasonic Humidifier) and monitored moisture with a humidity detector (DOQAUS Indoor Mini Digital Hygrometer Room with Thermometer and Humidity Meters). We used fresh cotton two-ply masks (ATA Reusable SILVADUR 930 FLEX, model MK100SS-11) for our study of the effect of masks on exhaled respiratory droplets. We delivered water droplets with the varying concentration of sodium and calcium chloride salts in our studies with a hand-held, vibrating-mesh nebulizer described elsewhere[38] using a 6-μm pore size to produce, on tipping of the device, an aerosol cloud with a median volume droplet diameter of 9–10 μm[38], optimal for nasal and upper airway deposition of aerosol following a deep natural tidal inspiration through the nose and with relatively uniform distribution of deposition from the anterior to the posterior of the nose. The device delivers a total mass dose of 57 mg +/– 2 mg within a 10-second actuation.

In our exhaled aerosol experiments, we had two exclusion criteria[1]. *Broken Seal*. Exhaled aerosol particle numbers recorded on the Climet particle counter in all circumstances within the parameters of our studies descended from the start of a human subject recording (when exhaled aerosol is largely a measure of the particle counts in the room) to the end of a human subject recording (when exhaled aerosol is a measure of the particle counts generated in the subject's own respiratory system). As described previously once exhaled aerosol

particle numbers reached a relatively consistent asymptote level, we counted three to eight 6-second averages as reported by the Climet detector and averaged these 6-second averages to obtain the exhaled aerosol number +/– standard deviation. We excluded those data where exhaled aerosol numbers once in this plateau period of time exceeded by more than 2 standard deviations the mean value of the exhaled aerosol number — deducing that a break in the participant's seal with the detector occurred (either at the lips or with the pinch of the nose)[2]. *Inadequate Equilibration*. Participants began each study by spending 2 hours in the dry (10% RH) room environment before the measurement of their baseline data. This period of time was critical to ensure that their exhaled aerosol numbers reflected the humidity conditions of the 10% RH room. In those cases where an individual began the study without the full 2-hour equilibration, we omitted their data from the study. Of the total 49 human subject tests, we excluded data from 6 human subject tests.

COVID-19 incidence and deaths versus proximity to US coastlines

We used an ecological regression model recently published[39] to analyze the relationship of county-level COVID-19 cases and deaths per capita over the cumulative course of the COVID-19 pandemic from January 2020 through March 2021. We sourced COVID 19 cases and death counts from the *New York Times* "Coronavirus in the U.S." county trends data[40]. These publicly accessible data are sourced from state and local health agencies across the United States[41]. We sourced population estimates for counties (FIPS regions) from the U.S. Census Bureau's County Population Estimates program[41] (released in March 2020). These data are provided by the Bureau's Population Division. We sourced county estimates of population density (population per square mile) from the 2010 Census, the most recent available cumulative Census. We sourced socioeconomic indicators within counties from the U.S. Census Bureau's Small Area Income and Poverty Estimates (SAIPE) program. This program analyzes data from the 2019 vintage of the American Community Survey (ACS) conducted annually. Socioeconomic indicators analyzed include poverty rates, youth poverty rates (i.e., poverty rates for residents < 18 years old), and median income. We sourced county-level 2012 climate zones according to the International Energy Conservation Code (IECC) from the U.S. Department of Energy, Office of Scientific and Technical Information[42]. Of the three moisture regimes defined in the IECC climate regions we interpreted those classified as moist or marine as high humidity areas for our analysis. We coded counties by proximity to relevant coastlines (coastal counties border the sea) using FIPS maps made available by the U.S. National Weather Service (NWS)[43]. For our data analysis reported we examined data for March 29, 2021, representing the cumulative count of cases and deaths by county from first reported 2020 up through this date. We sourced data on obesity by county from County Health Rankings, a project managed by University of Wisconsin Population Health Institute[44]. We sourced median age of U.S. citizens within U.S. counties from the U.S. Census Bureau's ACS, 2019 vintage 5-Year Estimates Subject Tables[45]. These estimates are based on data collected over a 5-year period of time for all geographic areas. We sourced political identity by U.S. county using the 2020 US Presidential election outcomes at the county level from *The New York Times*, *Fox News*, and *Politico*, using a web-scraper to aggregate results accessed via GitHub[46]. We sourced airborne fine particulate matter ($PM_{2.5}$) concentrations from Atmospheric Composition Analysis Group for 2018[47]. The annual mean $PM_{2.5}$ estimates are provided at $0.01° \times 0.01°$ grid resolution across the entire continental United States by fusing $PM_{2.5}$ measures from three different sources: ground-based monitors, GEOS-Chem chemical transport models (CTM), and satellite observations. These estimates have been extensively cross-validated, and the cross-validated R^2 for these models in the United States was reported to be 0.61, although the accuracy varies across regions. We aggregated these $PM_{2.5}$ estimates spatially by averaging across grid cells in each county. We relied on Python-based implementation of NUMPY[48] and PANDAS[49], R software version 3.5.1, and Microsoft Excel to enable this analysis. We used ThinkCell to construct Figures 1 and 2 and associated figures in the Supplemental Material.

Outcomes

Our outcome in the exhaled aerosol experiments was exhaled aerosol particle counts. The Climet 450-t particle counter reports particle counts as a function of aerodynamic particle size ranges for particles larger than 0.3 μm, particles larger than 0.5 μm, particles larger than 1 μm, and all particles larger than 5 μm. The numbers reported represent average values of particle counts automatically measured by the light-scattering detector over 6 seconds. For our determination of exhaled aerosol particle number we averaged three to eight average particle counts (each integrating a 6-second interval) as reported by the particle detector to determine the mean exhaled particle count and the standard deviation. Our outcome in the COVID-19 ecological study was cumulative COVID-19 cases and deaths per capita by COVID-19 as a function of coastal versus inland counties in the United States between January 1, 2020, and March 29, 2021.

Statistical analysis

All error bars represent 95% confidence intervals based on standard deviation values. Significance of differences in

individual and collective aerosol numbers was determined by two-tailed *t*-test. We calculated statistical significance of differences using a multiway analysis of variance (ANOVA) test for each set of variables. This allowed for evaluating the influence of multiple factors on the mean within a 95% confidence interval. *P*-values were calculated for each unique set of variables compared to baseline values. Each *P*-value below 0.05 was considered to be statistically different.

Role of the funding source

The study was funded by Sensory Cloud Inc. (Cambridge, MA) and in part by the Intramural Research Program of the NIH, The National Institute of Diabetes and Digestive and Kidney Diseases (NIDDK) (DK075154). This research was also supported by the Harvard University Climate Change Solutions Fund; the 2020 Star Friedman Challenge for Promising Scientific Research, for "Air pollution, race, and health outcomes for COVID-19 in the United States: data access, methods, and dissemination. The funders had no role in study design, data collection, data analysis, data interpretation, writing of the article, or the decision to publish the study. Participation of NIH in the funding of this research does not represent an endorsement of any product or service by Sensory Cloud.

RESULTS

In a first arm of our randomized control study, human subjects sat in an office at room temperature (20°C) for 2 hours with normal tidal breathing of air at 10% RH, then moved to an office humidified to 40% RH at the same temperature for 20 minutes, after which they returned to the dry office at 10% RH where they remained for 2 hours. Exhaled aerosol results are shown in Figure 1a. Numbers of exhaled aerosol particles for all subjects ($n = 8$) diminish ($P < 0.05$) following 10 minutes of breathing the moist air relative to the "baseline" exhaled aerosol, the latter reflecting 2 hours breathing of the dry air. Exhaled aerosol continues to diminish through 20 minutes

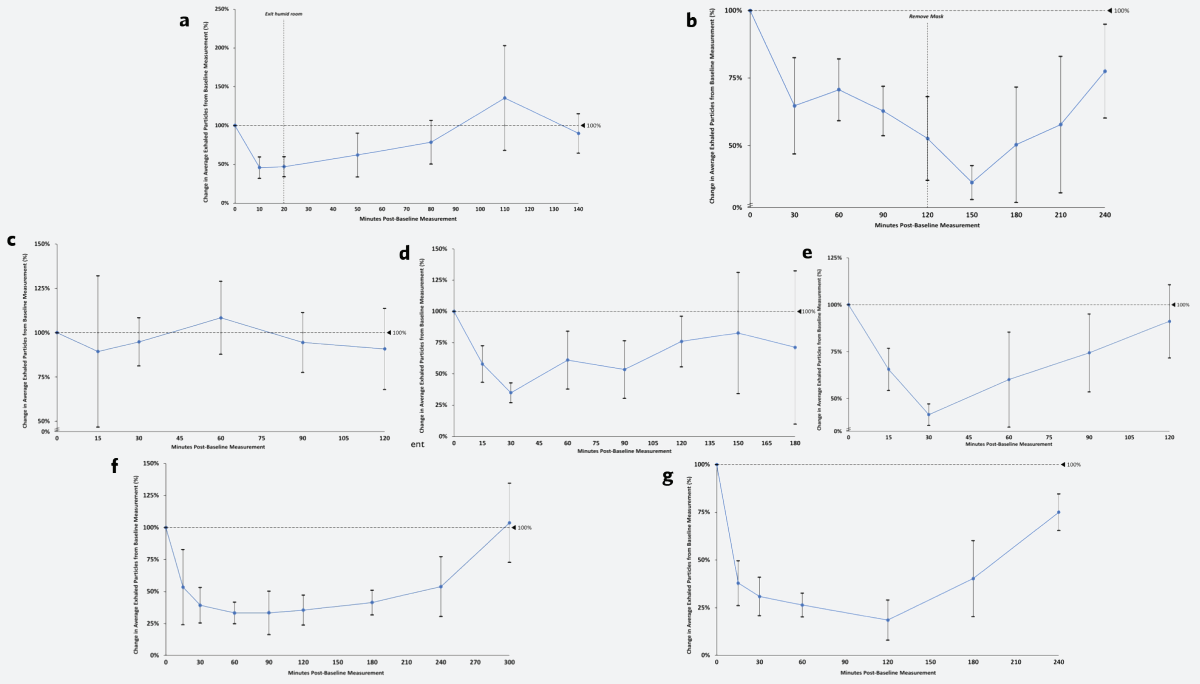

Figure 1. Exhaled aerosol measured at 10% RH and 20°C during the normal tidal breathing of human subjects as a function of time in seven protocols that altered the moisture and salt content of inhaled air. (a) Subjects breathed humid air (40% RH at 20°C) for 20 minutes post baseline exhaled aerosol after which they returned to the dry room (10% RH at 20°C). (b) Subjects breathed through cotton masks for 120 minutes post baseline exhaled aerosol after which they returned to the dry room (10% RH at 20°C). (c) Subjects nasally inhaled a pure water mist post baseline exhaled aerosol after which they remained in the dry room (10% RH at 20°C). (d) Subjects nasally inhaled a water mist with 0.9% sodium chloride (isotonic saline) post baseline exhaled aerosol after which they remained in the dry room (10% RH at 20°C). (e) Subjects nasally inhaled a water mist with 5.0% sodium chloride (hypertonic saline) post baseline exhaled aerosol after which they remained in the dry room (10% RH at 20°C). (f) Subjects nasally inhaled a water mist with 5.0% calcium chloride post baseline exhaled aerosol after which they remained in the dry room (10% RH at 20°C). (g) Subjects nasally inhaled a water mist with 5.0% magnesium chloride post baseline exhaled aerosol after which they remained in the dry room (10% RH at 20°C).

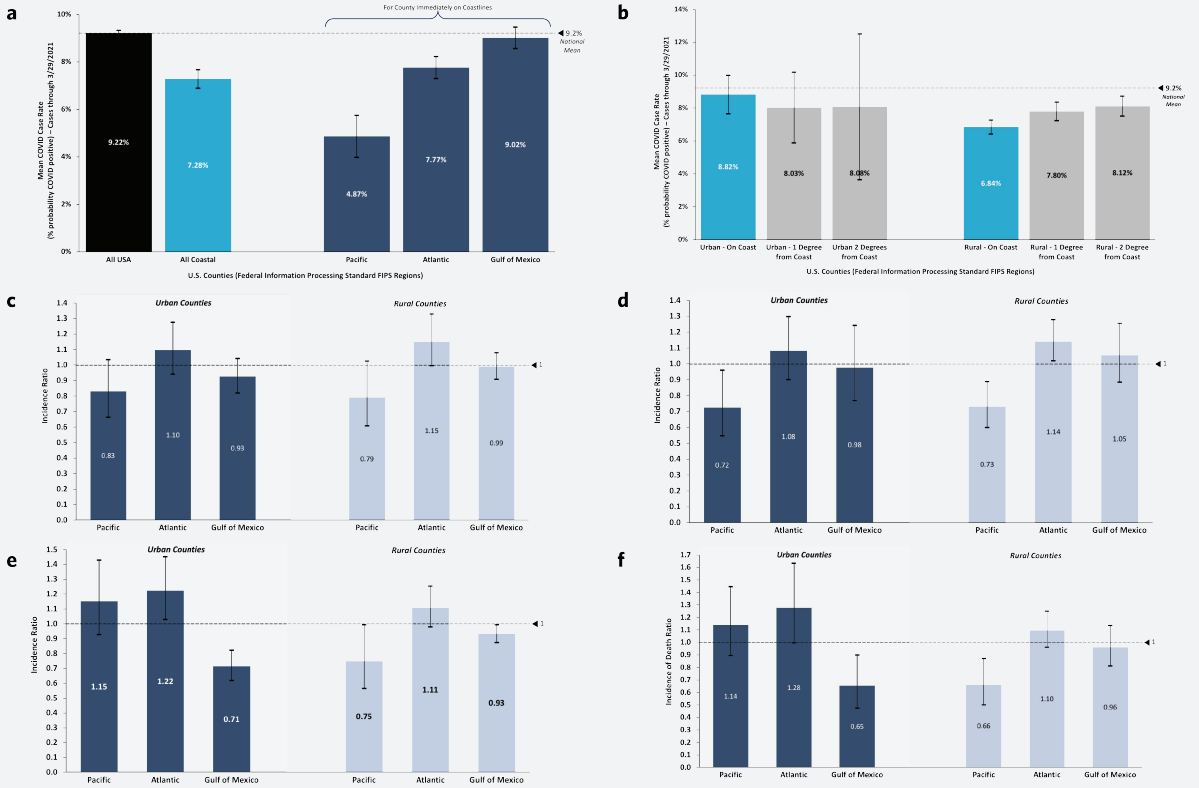

Figure 2. COVID-19 cases and deaths per county in the United States since the start of the pandemic through March 29, 2021, as a function of coastal and inland geographies. (a) Cases per capita for United States, Coastal (counties abutting the sea), and Pacific, Gulf, and Atlantic Coasts. (b) Deaths per capita for United States, Coastal (counties abutting the sea), and Pacific, Gulf, and Atlantic Coasts. (c) Coastal relative to inland cases per capita by ecological regression analysis assessing the effect of humidity and airborne salt while controlling for other confounding variables. (d) Coastal relative to inland deaths per capita by ecological regression analysis assessing the effect of humidity and airborne salt while controlling for other confounding variables. (e) Coastal relative to inland cases per capita by ecological regression analysis assessing the effect of airborne salt alone while controlling for other confounding variables including humidity. (f) Coastal relative to inland deaths per capita by ecological regression analysis assessing the effect of airborne salt alone while controlling for other confounding variables including humidity. All source data from NYTimes Covid Tracker Data (via GitHub); United States Census Bureau; IECC/energy.gov. Counties (FIPS regions) are classified by IECC as hot-humid, mixed-humid, and marine.

in the humid room to approximately 50% of baseline levels ($P < 0.05$). On return to the dry room after 20 minutes in the humid room, exhaled aerosol numbers increase, returning to baseline 60 minutes post departure from the humid office ($P = 0.110$).

In a second arm, subjects sat in a dry office at room temperature (20°C) for 2 hours as in the first protocol, then wore a cotton face mask in the same office for an additional 2 hours, after which they removed the mask and continued to breathe the dry air for the next 2 hours. The results are shown in Figure 1b. Exhaled aerosol for all subjects ($n = 9$) diminishes over the 2 hours of mask wearing relative to the baseline exhaled aerosol assessed after breathing the dry air ($P < 0.05$)[37]. On removal of the mask in the dry room, exhaled aerosol increases, remaining significantly low at 60 minutes post mask removal ($P < 0.05$) and returning to baseline between 90 minutes ($P < 0.05$) and 120 minutes ($P = 0.542$) post removal of the mask. The effect of the (2 hour wearing of the) mask on respiratory droplet generation (Figure 1b) is similar to the effect of the (20 minutes) breathing humid air (Figure 1a).

In a third arm, subjects sat in a dry office as in the first two protocols, then breathed in via the nose a mist of water droplets of 9–10 μm average diameter, sized to deposit in the nose, trachea, and main bronchi[32], via a hand-held vibrating mesh generator. Nasal inhalation of droplets was repeated with droplets containing isotonic saline (0.9% by weight sodium chloride) and hypertonic saline (5.0% by weight sodium chloride). The results are shown in Figures 1c–1e. On the delivery of distilled water droplets (Figure 1c), exhaled aerosol is statistically unchanged at all assessed time points post inhalation ($P = 0.343$). In the case of isotonic saline

Table 1. Estimates of airborne water and salt effects on COVID-19 incidence and death ratios for (urban and rural) coastal counties of the United States relative to (urban and rural) inland counties based on an ecological regression analysis[39] normalizing by confounding factors and assessing their sensitivity to estimates made

Cases (urban)				Deaths (urban)			
Predictors	Incidence rate ratios	CI	p	Predictors	Death rate ratios	CI	p
(Intercept)	0.090	0.085–0.096	**< 0.001**	(Intercept)	0.002	0.001–0.002	**< 0.001**
regionatlantic	1.096	0.942–1.275	0.237	regionatlantic	1.082	0.901–1.298	0.399
regiongulf of mexico	0.925	0.820–1.043	0.202	regiongulf of mexico	0.977	0.769–1.242	0.851
regionpacific	0.829	0.663–1.036	0.100	regionpacific	0.723	0.546–0.959	**0.025**
scale(popdensity)	0.979	0.931–1.031	0.426	scale(popdensity)	1.026	0.947–1.113	0.525
scale(poverty)	0.994	0.856–1.155	0.940	scale(poverty)	1.218	1.027–1.444	**0.024**
scale(log(median_income))	0.964	0.854–1.087	0.549	scale(log(median_income))	1.096	0.913–1.316	0.324
scale(pct_obesity)	1.025	0.940–1.117	0.582	scale(pct_obesity)	1.097	0.970–1.240	0.140
scale(voter_margin_2020)	1.148	1.105–1.193	**< 0.001**	scale(voter_margin_2020)	1.101	1.013–1.197	**0.024**
scale(median_age)	0.957	0.881–1.040	0.299	scale(median_age)	1.301	1.184–1.429	**< 0.001**
factor(party)Republican	1.054	0.878–1.265	0.573	factor(party)Republican	1.036	0.778–1.379	0.811
scale(mean_pm25)	1.012	0.936–1.093	0.773	scale(mean_pm25)	0.986	0.861–1.129	0.839
scale(mean_summer_rm)	0.932	0.885–0.982	**0.009**	scale(mean_summer_rm)	0.902	0.832–0.978	**0.013**
scale(mean_winter_rm)	0.910	0.859–0.964	**0.001**	scale(mean_winter_rm)	0.879	0.800–0.965	**0.007**
Observations	86			Observations	86		
Cases (rural)				**Deaths (rural)**			
Predictors	Incidence rate ratios	CI	p	Predictors	Death rate ratios	CI	p
(Intercept)	0.091	0.084–0.099	**< 0.001**	(Intercept)	0.002	0.002–0.002	**< 0.001**
regionatlantic	1.151	0.996–1.330	0.057	regionatlantic	1.141	1.019–1.279	**0.022**
regiongulf of mexico	0.991	0.909–1.080	0.829	regiongulf of mexico	1.054	0.885–1.255	0.554
regionpacific	0.790	0.608–1.026	0.077	regionpacific	0.731	0.600–0.889	**0.002**
scale(popdensity)	1.025	1.008–1.042	**0.005**	scale(popdensity)	1.022	0.994–1.052	0.129
scale(poverty)	0.986	0.919–1.058	0.697	scale(poverty)	1.186	1.055–1.334	**0.004**
scale(log(median_income))	0.918	0.871–0.967	**0.001**	scale(log(median_income))	0.947	0.839–1.070	0.383
scale(pct_obesity)	0.987	0.935–1.042	0.638	scale(pct_obesity)	1.038	0.996–1.083	0.079
scale(voter_margin_2020)	1.115	1.057–1.177	**< 0.001**	scale(voter_margin_2020)	1.121	1.053–1.193	**<0.001**
scale(median_age)	0.893	0.864–0.924	**< 0.001**	scale(median_age)	1.099	1.026–1.177	**0.007**
factor(party)Republican	1.006	0.942–1.074	0.860	factor(party)Republican	0.906	0.821–0.999	**0.048**
scale(mean_pm25)	1.032	0.989–1.076	0.153	scale(mean_pm25)	1.047	0.979–1.119	0.181
scale(mean_summer_rm)	0.987	0.947–1.028	0.525	scale(mean_summer_rm)	1.017	0.940–1.100	0.675
scale(mean_winter_rm)	0.963	0.920–1.007	0.102	scale(mean_winter_rm)	0.918	0.862–0.978	**0.008**
Observations	3014			Observations	3014		

(Figure 1d), average exhaled aerosol decreases to about half the baseline levels for most subjects at 30 minutes ($P < 0.05$), returning to baseline within 60 minutes post inhalation ($P = 0.057$), closely mimicking the experience of breathing humid air (Figure 1a). In the case of hypertonic saline (Figure 1e), exhaled aerosol diminishes post inhalation again to about half the baseline levels at 30 minutes ($P < 0.05$) and returns to baseline for all subjects ($n = 8$) within 90 minutes

Table 2. Estimates of airborne salt effects on COVID-19 incidence and death ratios for (urban and rural) coastal counties of the United States relative to (urban and rural) inland counties based on an ecological regression analysis[39] Normalizing by confounding factors — including relative humidity — and assessing their sensitivity to estimates made

Cases (urban)				Deaths (urban)			
Predictors	Incidence rate ratios	CI	p	Predictors	Death rate ratios	CI	p
(Intercept)	0.090	0.083–0.098	**< 0.001**	(Intercept)	0.002	0.001–0.002	**< 0.001**
regionatlantic	1.223	1.029–1.453	**0.023**	regionatlantic	1.275	0.995–1.634	0.055
regiongulf of mexico	0.713	0.619–0.821	**< 0.001**	regiongulf of mexico	0.654	0.475–0.900	**0.009**
regionpacific	1.151	0.927–1.428	0.203	regionpacific	1.138	0.895–1.446	0.292
scale(popdensity)	0.988	0.930–1.049	0.684	scale(popdensity)	1.032	0.910–1.171	0.623
scale(poverty)	0.964	0.790–1.175	0.715	scale(poverty)	1.180	1.008–1.382	**0.040**
scale(log(median_ income))	0.839	0.642–1.097	0.199	scale(log(median_ income))	0.913	0.665–1.255	0.575
scale(pct_obesity)	0.930	0.815–1.061	0.280	scale(pct_obesity)	0.955	0.786–1.160	0.640
scale(voter_ margin_2020)	1.131	1.046–1.223	**0.002**	scale(voter_ margin_2020)	1.084	1.002–1.172	**0.044**
scale(median_age)	0.926	0.838–1.024	0.134	scale(median_age)	1.232	1.093–1.389	**0.001**
factor(party) Republican	0.979	0.810–1.183	0.825	factor(party) Republican	0.928	0.642–1.341	0.691
scale(mean_pm25)	0.977	0.879–1.087	0.671	scale(mean_pm25)	0.945	0.828–1.080	0.408
Observations	86			Observations	86		
Cases (rural)				**Deaths (rural)**			
Predictors	Incidence rate ratios	CI	p	Predictors	Death rate ratios	CI	p
(Intercept)	0.097	0.089–0.107	**< 0.001**	(Intercept)	0.002	0.002–0.002	**< 0.001**
regionatlantic	1.109	0.980–1.254	0.102	regionatlantic	1.096	0.962–1.250	0.169
regiongulf of mexico	0.932	0.874–0.944	**0.033**	regiongulf of mexico	0.960	0.812–1.134	0.627
regionpacific	0.749	0.565–0.993	**0.045**	regionpacific	0.661	0.501–0.871	**0.003**
scale(popdensity)	1.016	0.996–1.036	0.113	scale(popdensity)	1.012	0.981–1.044	0.444
scale(poverty)	1.011	0.945–1.082	0.741	scale(poverty)	1.237	1.091–1.402	**0.001**
scale(log(median_ income))	0.942	0.893–0.994	**0.028**	scale(log(median_ income))	0.991	0.863–1.137	0.894
scale(pct_obesity)	0.970	0.930–1.012	0.154	scale(pct_obesity)	1.023	0.979–1.069	0.308
scale(voter_ margin_2020)	1.128	1.070–1.190	**< 0.001**	scale(voter_ margin_2020)	1.138	1.066–1.214	**< 0.001**
scale(median_age)	0.883	0.854–0.913	**< 0.001**	scale(median_age)	1.086	1.008–1.171	**0.031**
factor(party) Republican	0.956	0.882–1.036	0.268	factor(party) Republican	0.846	0.755–0.947	**0.004**
scale(mean_pm25)	1.022	0.978–1.068	0.334	scale(mean_pm25)	1.030	0.955–1.111	0.442
Observations	3014			Observations	3014		

($P = 0.746$) (Figure 1e), similar to the wearing of the cotton mask for 2 hours (Figure 1b).

In a fourth arm, we replaced sodium chloride by calcium chloride or magnesium chloride. We followed the same protocol as in the third study. Figures 1f and 1g show the results. Exhaled aerosol diminishes post nasal inhalation and remains significantly suppressed for all subjects in both cases through 3 hours ($P < 0.05$) post inhalation before returning to baseline at 4 hours for magnesium chloride ($P = 0.11$), while for calcium chloride counts remain suppressed ($P < 0.05$), returning to baseline at 5 hours for the calcium aerosol ($P = 0.999$), a significantly longer suppression of respiratory droplet generation than observed following humidity change (Figure 1a), mask wearing (Figure 1b), and sodium chloride salt (Figures 1d and 1e) exposure. Individual exhaled aerosol counts and twin-tailed *t*-test results for all subjects in all of the four protocols are shown in the Supplemental Material.

We preliminarily explored whether prolonged exposure to high airborne salt and water in the United States over the course of the COVID-19 pandemic might associate with significant differences in COVID-19 incidence or symptoms (death). Figure 2a presents COVID-19 cases per capita in those counties immediately bordering the US coastlines compared to the total national cases per capita. COVID-19 per capita cases are approximately 21% lower than the national mean along US coastlines ($P < 0.05$), and approximately 47% lower ($P < 0.05$) along the Pacific Coast. Figure 2b presents deaths per COVID-19 cases per capita. COVID-19 deaths are suppressed ($P < 0.05$) by 15% relative to the national mean along the coastal regions of the United States, an outcome entirely due to very low death rates in counties bordering the Pacific Coast (53% lower than the national mean). See Supplemental Material for further detail on our evaluation of statistical significance of differences.

To explore whether low coastal COVID-19 incidence and death rates associate with high airborne salt and humidity exposure or other potentially confounding factors, including age, economic circumstances, voting patterns, population density, and air pollution — we used an ecological regression analysis (19) adjusting for a combination of 10 potentially confounding socioeconomic, phenotypical and environmental variables including humidity (see Supplemental Material).

The results of our analysis are shown in Tables 1 and 2 and Figures 2c–2f. Figures 2c and 2d compare the estimated influence of airborne salt and moisture combined on the ratio of COVID-19 incidence and death rates per capita for urban and rural coastal counties relative to inland counties. Comparing urban coastal and inland regions including both water and salt exposure effects, there is no statistical change in incidence of COVID-19 on any US coast accounting for all confounding factors, while death rate is significantly suppressed along the Pacific Coast in rural coastal communities (27%, $P = 0.003$) and with lesser significance in urban communities (28%, $P = 0.045$), reflecting the high airborne salt exposure along the Pacific Coast and the confounding variable of urban population density. Figures 2d and 2e indicate that the effect of salt exposure alone suppresses incidence of COVID-19 by 29% on the Gulf Coast ($P < 0.001$), and Gulf Coast death rate by 35% ($P = 0.033$), while in rural counties no effect appears on death rate ($P = 0.662$) and incidence is marginally suppressed by 7% ($P = 0.033$), corresponding to high airborne salt due to strong winds off the sea notably along the Texas panhandle where the greatest urban population exists on the Gulf Coast (Supplemental Material). Comparing rural coastal and inland regions, incidence of COVID-19 is suppressed by 25% on the Pacific Coast ($P = 0.045$), and Pacific Coast death rate by 34% ($P = 0.003$), while no significant effect appears in urban counties ($P > 0.05$), where population density is greater (4773 residents per square mile) than in Gulf Coast urban coastal communities (2593 residents per square mile), and airborne salt exposure is highest owing to strong winds off the sea all along the coast (Supplemental Material).

DISCUSSION

Our results show for the first time that the hydration of the upper airways can rapidly and significantly alter respiratory droplet generation, a phenomenon that has received unprecedented attention over the last year for its role in the airborne transmission of COVID-19[3,36], and, consequently, that variation in upper airway respiratory droplet numbers might be a factor in the reported impact of environmental humidity on symptoms of COVID-19[14] and other respiratory diseases[13].

We find that respiratory droplet generation on normal tidal breathing varies inversely with airway hydration, growing on the breathing of dry air, and diminishing on the breathing of either moist air (Figure 1a) or salts (Figures 1d, 1e, and 1f). This hydration-dependent variance of respiratory droplet generation impacts the normal clearance function of upper airway lining mucus in a similar way as does the hydration dependent variance of cilia beat frequency[20]. Higher numbers of respiratory droplets increase the probability that foreign contaminants within mucus, rather than being cleared toward the mouth through the action of cilia beat, return to the air and penetrate deeper into the lungs (or get exhaled into the environment). This breakdown of the normal clearance function of airway mucus is similar in consequence to the breakdown of clearance that occurs on the slowing down of cilia beat, which has long been recognized to occur on the drying out of the airways[7–10]. This dependence of respiratory droplet generation on hydration of the airways has direct relevance to respiratory health[10–14].

While respiratory droplet generation can be caused by the necking of airway lining fluid in the small airways[50],

a phenomenon we particularly observe with forced expiratory and inspiratory volume inhalation and exhalation (see Supplemental Material), our results show that normal tidal breathing leads to respiratory droplet generation principally in the upper airways (Figures 1d, 1e and 1f), where air is hydrated on inhalation prior to penetrating the lungs. Such upper airway droplet generation occurs by the way of the shear force of air flowing across mucus surfaces in the trachea and main bronchi[26,27,31]. Typical maximal air speeds through trachea and main bronchi during normal tidal breathing are 2 m/s[25], while far higher air speeds occur in the vicinity of the carina on normal tidal inhalation as a consequence of the jet of air that forms on air passage through the larynx[25]. Peak air speeds on inhalation and exhalation at or above air speeds (2 m/s) are found to generate significant mists of salt water over the sea[15]. During the course of breathing, inhaled and exhaled air creates microscopic waves, analogous to sea waves. Wave undulations are known to increase in number and break more easily into mist with increasing surface elasticity[26], a property highly dependent on the presence of surface active material, which in mucus includes lung surfactants[27], as preliminary, and small hydrophobic particles that may have deposited from the external air on inhalation[28]. Further promoting greater undulations of fluid surfaces are increases in the fluidity and elasticity of underlying fluid, as can occur with the loss of glycosylated mucin coat that can occur with aging and poor diet[51]. The dimension of the undulations, and therefore droplet size, is strongly dependent on surface tension, again varying with the presence or absence of surface-active material.

With the breathing of dry air, upper airway lining fluid volume shrinks, nonvolatile components increase in concentration, and this increases surfactant concentration at mucus surfaces. The exchange of surfactant on mucus surfaces promotes greater droplet generation[31]. Breathing humid air leads to less evaporation from the airway lining fluid, increasing the thickness of the airway lining fluid layer and thereby lowering surfactant concentration, thus resulting in fewer droplets. As shown in Figure 1a, drying out of upper airway mucus leads to more respiratory droplets, not less, while humidifying the upper airways leads to fewer droplets, not more. That the wearing of cotton masks promotes the same phenomenon is consistent with the recent report that masks humidify inhaled air[37] and suggests that humidification of the upper airways may be one of the reasons mask-wearing, and notably the wearing of cotton masks, has proven as beneficial as it has during the COVID-19 pandemic[52].

With the breathing of salt, osmotic pressure grows across the membranes of epithelial cells in the upper airways and pulls water into the airway lining fluid, hydrating the airways as otherwise occurs when the airways are dehydrated. In our experiments, we delivered salt to the upper airways with a handheld nebulizer that delivered approximately 20 mg solution per inhalation[38]. Total volume of fluid in the trachea (approximately 10 cm in length, approximately 2 cm diameter, approximately 10 μm in thickness) is approximately 60 mg. Nasal inhalation of the mist therefore appreciably alters water volume in the upper airways, and therefore salt balance. The consequent expansion of airway lining fluid volume reduces surfactant concentration, an effect that mirrors the effect of the breathing of humid air (compare Figures 1a and 1d and 1e). That this (upper airway targeted) aerosolized saline effect (Figures 1d and 1e) so closely mimics in duration and extent of the humidity effect (Figure 1a) strongly suggests the upper airways as a primary site of respiratory droplet generation on normal breathing; that the delivery of pure water droplets (Figure 1c) to the same site has no effect even though "hydrating the airways" reflects the osmotic nature of the natural hydration process, which appears to rapidly pull water out of the airway lining fluid driven by the dilution effect of the salt-free water.

While we view our findings that the high levels of airborne salt and humidity along the US coastlines — notably along the Gulf Coast (where inland coastal winds are strong particularly on the Texas panhandle) and the Pacific Coast (where inland coastal winds are high along most of the coastline) — significantly reduce he incidence of COVID-19 and deaths (Figures 1c–1f), the findings are at least consistent with the environmental variables on the Gulf and Pacific Coasts as with our human volunteer study findings. Estimates of salt concentrations in the air along seacoasts vary depending on wind speed and orientation. Airborne salt concentrations over the ocean surface can range between (salt volume to air volume) 2 and 6 $\mu m^3/cm^3$ notably as a consequence of sea spray aerosols generated by wind speeds of 2–20 m/s[15]. Similar concentrations have been measured within 10 m of the ground within approximately 500 m from the coastline with wind speeds of 2 m/s or greater and oriented inland[16]. These masses of airborne salt, consistent with average wind speeds and orientations along the Pacific Coast (Supplemental Material), equate to masses of airborne salt ranging from 0.006 to 0.02 μg of salt per liter of air. A day of normal breathing (assuming 1 liter per breath, 10 breaths per minute) of such salty air results in the inhalation of around 60–200 μg of salt per day. The breathing of 60–200 μg of salt per day is equivalent to a single inhalation of approximately 1–4 mg of a 5% solution of hypertonic saline, which is near the mass of salt solution nasally inhaled in the experiments whose results are shown in Figures 1c–1f[33]. In the absence of strong inland-oriented winds off the sea, airborne salt concentrations are more difficult to estimate, while chloride deposition on the ground, commonly monitored for its relevance to corrosion potential, is generally elevated along seacoasts — and in the United States extends significantly inland on all coasts largely due to rainfall[17].

Mechanistically, the effects of inhaled moist, salty air on COVID-19 incidence and symptoms need further study. The breathing of moist, salty air may lower the transmission potential of SARS-CoV-2 by lowering respiratory droplet exhalation, acting in this sense as a mask, a phenomenon previously observed in a porcine influenza model[33], where airborne transmission of influenza between porcine in widely separated cages was blocked by the delivery of salted droplets to porcine lungs. Diminished transport potential of virus from the upper airways to the lower respiratory tract and the enhancement of cilia clearance in the upper airways may, on the other hand, each account for a reduction of COVID-19 symptoms by the breathing of moist salty air. These same phenomena appear to underly the results of a recent randomized control study[53] of 40 COVID-19 patients infected with SARS-CoV-2 and treated for three days post detection, where delivery of a hypertonic calcium-rich saline of similar composition as the 5% calcium chloride aerosol used in the present human volunteer study significantly reduced symptoms of COVID-19 relative to a control of nasal (isotonic) saline spray.

The results of this study raise questions as to the respective roles on respiratory disease of respiratory droplet suppression and enhanced cilia beat frequency following the upper airway delivery of hypertonic salts, and their relationship to environmental factors in the modulation of respiratory disease. Practically, the safety, naturalness, and ease of access of exposure to moist, salty air, suggests that a range of approaches to upper airway hydration might be encouraged to improve respiratory health and well-being, ranging from the breathing of moderately humid air, to prolonged exposure to sea air, or the daily inhalation of hypertonic calcium- or magnesium-rich salt droplets sized to deposit in the nose and upper airways. Airway hygiene seems a special opportunity today given the realities of the COVID-19 pandemic and the longer-term global crisis of dirty air[6].

CONFLICT OF INTEREST

David Edwards is the Founder, a board member, and a shareholder of Sensory Cloud; Dr Dennis Ausiello is a board member and a shareholder of Sensory Cloud; Jonathan Salzman is an employee of Sensory Cloud. Sensory Cloud, Inc., was one of the funders of the study while all data were gathered and interpreted with researchers at independent institutions so that no organization's researchers solely gathered and interpreted the study data.

ACKNOWLEDGMENTS

The authors thank Pia MacDonald (RTI) for her helpful comments following a critical read of an early manuscript as well as helpful feedback from Peter Small (Stony Brook), John Brownstein (Harvard Medical School), and Tony Hickey (UNC).

REFERENCES

1. Shelly, M.P. The upper airway — the forgotten organ. *Crit. Care* **5**(1), 1–2 (2001). doi:10.1186/cc971.
2. Lawal, O., Ahmed, W.M., Nijsen, T.M.E., Goodacre, R. & Fowler, S.J. Exhaled breath analysis: a review of 'breath-taking' methods for off-line analysis. *Metabolomics* **13**(10), 110 (2017). doi:10.1007/s11306-017-1241-8.
3. Zhang, R., Li, Y., Zhang, A.L., Wang, Y. & Molina, M.J. Identifying airborne transmission as the dominant route for the spread of COVID-19. *Proc. Nati. Acad. Sci* **117**(26), 14857–14863 (2020).
4. Heyder, J. Deposition of inhaled particles in the human respiratory tract and consequences for regional targeting in respiratory drug delivery. *Proc. Am. Thorac. Soc.* V **104**, 315–320 (2004).
5. Moriyama, M., Hugentobler, W.J. & Iwasaki, A. Seasonality of respiratory infections. *Annu. Rev. Virol* **7**(1), 83–81 (2020).
6. Meghlji, J. Improving Improving lung health in low-income and middle-income countries: from challenges to solutions. *Lancet* **397**(10277), P928–P940 (2021).
7. Argyropoulos, C. *et al*. Hypertonicity: pathophysiologic concept and experimental studies. *Cureus* **8**(5), e596 (2016). doi:10.7759/cureus.596
8. Even-Tzur, N. *et al*. Climate chamber for environmentally controlled laboratory airflow experiments. *Technol. Health. Care* **18**, 157–163 (2010).
9. Barbet, J.P., Chauveau, M., Labbe, S. & Lockhart, A. Breathing dry air causes acute epithelial damage and inflammation of the guinea pig trachea. *J. Appl. Physiol.* **64**, 1851–157 (1988).
10. Kudo, E. *et al*. Low ambient humidity impairs barrier function and innate resistance against influenza infection. *PNAS* **116**, 10905–10910 (2019).
11. D'Amato, M. *et al*. The impact of cold on the respiratory tract and its consequences to respiratory health. *Clin. Transl. Allergy* (2018). doi:10.1186/213601-018-0208-9.
12. Ghosh, A., Boucher, R.C. & Tarran, R. Airway hydration and COPD. *Cell. Mol. Life. Sci.* **72**(19), 3637–3652 (2015). doi:10,1007/s00018-015-1956-7.
13. Kudo E. *et al*. Influenza worsens dry air Low ambient humidity impairs barrier function and innate resistance against influenza infection. *Proc. Nati. Acad. Sci*. **116**(22), 10905–10910 (2019). doi:10.1073/pnas.1902840116

14. Mecenas, P., Bastos, R., Vallinoto, A. & Normando, D. Effects of temperature and humidity on the spread of COVID-19: a systematic review. *PLOS ONE* **15**(9), e0238339 (2020). doi:10.1371/journal.pone.0238339.
15. Liu, S. *et al*. Sea spray aerosol concentration modulated by sea surface temperature. *Proc. Nati. Acad. Sci.* **118**(9), e2020583118 (2021). doi:10.1073/pnas.202058311.
16. Castañeda-Valdés, A., Corvo-Pérez, F., Howland, J.J. & Águila, R.M. Havana airborne salinity penetration in the coastal tropical climate of the Havana Cuba. *Revista. CENIC Ciencias. Químicas. Número. Especial* **46**, 90–99 (2015).
17. Slamova, K., Glaser, R., Schill, C., Wiesmeier, S. & Köhla, M. Mapping atmospheric corrosion in coastal regions: methods and results. *J. Photon. Energy* **2**, 022003-1 (2012).
18. Elkins, M.R. & Bye, P.T. Mechanisms and applications of hypertonic saline. *J. R. Soc. Med.* **104**(Suppl 1), S5 (2011). doi.10.1258/jsrm.2011.s11101
19. Kelly, J.S., Martinsen, P. & Tatkov, S. Rapid changes in mucociliary transport in the tracheal epithelium caused by unconditioned room air or nebulized hypertonic saline and mannitol are not determined by frequency of beating cilia. *Intensive. Care. Med. Exp.* **9**, 8 (2021). https://doi.org/10.1186/s40635-021-00374-y.
20. Bennett, W.D. *et al*. Duration of action of hypertonic saline on mucociliary clearance in the normal lung. *J. Appl. Physiol.* **118**, 1483–1490 (2015).
21. Reeves, E.R. *et al*. Hypertonic saline in treatment of pulmonary disease in cystic fibrosis. *Sci. World. J.* **2012**, 11 (2012). doi:10.1100/2012/465230
22. Kassel, J.C., King, D. & Spurling, G.K. Saline nasal irrigation for acute upper respiratory tract infections. *Cochrane. Database. Syst. Rev.* **17** (3), CD006821 (2010). doi:10.1002/14651858.CD006821.pub2. Update in: Cochrane Database Syst Rev. 2015;4:CD006821. PMID: 20238351.
23. Rashleigh, R., Smith, S.M. & Roberts, N.J. A review of halotherapy for chronic obstructive pulmonary disease. *Int. J. Chron. Obstruct. Pulmon. Dis.* **9**, 239–246 (2014). doi:10.2147/COPD.S57511. PMID: 24591823; PMCID: PMC3937102.
24. Chervinskaya, A.V. & Kotenko, K.V. Efficiency of controlled halotherapy in rehabilitation of patients with occupational lung diseases. *Med. Tr. Prom. Ekol* **11**, 38–40 (2016). English, Russian. PMID: 30351691.
25. Martonen, T.B., Zhang, Z. & Lessmann, R.C. Fluid dynamics of the human larynx and upper tracheobronchial airways. *Aerosol. Sci. Technol.* **19**(2), 133–156 (1993). doi:10.1080/02786829308959627
26. Moren, F. *Aerosols in Medicine: Principles, Diagnosis, and Therapy*. 2nd ed. (Elsevier 1993).
27. Watanabe, W. *et al*. Why inhaling salt water changes what we exhale. *J. Colloid. Interface. Sci.* **307**(1), 71–78 (2007).
28. Hamed, R., Schenck, D.M. & Fiegel, J. Surface rheological properties alter aerosol formation from mucus mimetic surfaces. *Soft. Matter* **16**(33), 7823–7834 (2020). doi:10.1039/d0sm01232g. PMID: 32756700.
29. Mei, Y., Li, G., Moldenaers, P. & Cardinaelsac, R. Surface elasticity wave formation breakup Dynamics of particle-covered droplets in shear flow: unusual breakup and deformation hysteresis. *Soft. Matter* **12**, 9407 (2016).
30. Linder, A. & Wagner, C. Surface viscoelastic surface instabilities. *C. R. Phys* **10**(8), 712–727 (2009).
31. Crowther, R.S. & Marriott, C. Counter-ion binding to mucus glycoproteins. *J. Pharm. Pharmacol* **36**(1), 21–26 (1984). doi:10.1111/j.2042-7158.1984.tb02980.x. PMID: 6141258.
32. Edwards, D.A. *et al*. Inhaling to mitigate exhaled bioaerosols. *Proc. Nati. Acad. Sci.* **101**(50), 17383–17388 (2004).
33. Edwards, D., Salzman, J., Devlin, T. & Langer, R. Nasal calcium-rich salts for cleaning airborne particles from the airways of essential workers, students, and a family in quarantine. *Mol. Front. J.* **4**(01n02), 36–45 (2020).
34. George, C.E. *et al*. Airway hygiene in children and adults for lowering respiratory droplet exposure in clean and dirty air. *Mol. Front. J.* **4**(01n02), 46–57 (2020).
35. Leung, N.H. *et al*. Respiratory virus shedding in exhaled breath and efficacy of face masks. *Nat. Med.* **5**, 676–680 (2020).
36. Morawska, L. & Milton, D.K. It is time to address airborne transmission of coronavirus disease 2019 (COVID-19). *Clin. Infect. Dis.* **71**(9), 2311–2313 (2020).
37. Courtney, J.M. & Bax, A. Hydrating the respiratory tract: an alternative explanation why masks lower severity of COVID-19. *Biophys. J.* **120**(6), 994–1000 (2021).
38. Edwards, D. *et al*. A new natural defense against airborne pathogens. *QRB. Discovery* **1** (2020).
39. Wu, X., Nethery, R.C., Sabath, M.B., Braun, D. & Dominici, F. Air pollution and COVID-19 mortality in the United States: strengths and limitations of an ecological regression analysis. *Sci. Adv.* **6**(45), eabd4049 (2020).
40. The New York Times. Coronavirus (Covid-19) data in the United States. https://github.com/nytimes/covid-19-data (2021)
41. Bureau, U. S. C. County Population Totals: 2010-2019. https://www. census. gov/data/tables/time-series/demo/popest/2010s-counties-total. html (2020).

42. Burleyson, C. IECC climate zones. United States: N. p., 2020. Web. 2012. doi:10.25584/data.2020-05.1197/1617637
43. NOAA. US Wind Climatology: National Centers for Environmental Information. https://www.ncdc.noaa.gov/societal-impacts/wind/
44. County Health Rankings [Internet]. University of Wisconsin Population Health Institute; 2021. Adult obesity; 2021 [cited]. https://www.countyhealthrankings.org/explore-health-rankings/measures-data-sources/county-health-rankings-model/health-factors/health-behaviors/diet-exercise/adult-obesity
45. U.S. Census Bureau. 2015-2019 American Community Survey 5-year estimates Subject Tables. https://www.census.gov/data/developers/data-sets/acs-5year.html (2019).
46. McGovern, T. United States General Election Presidential Results by County from 2008 to 2020 [Source code]. https://github.com/tonmcg/US_County_Level_Election_Results_08-20 (2020).
47. van Donkelaar, A., Martin, R.V., Li, V. & Burnett, R.T. Regional estimates of chemical composition of fine particulate matter using a combined geoscience-statistical method with information from satellites, models, and monitors. *Environ. Sci. Technol.* **53**, 2595–2611 (2019). County Health Rankings. https://www.countyhealthrankings.org/explore-health-rankings/measures-data-sources/county-health-rankings-model/health-factors/health-behaviors/diet-exercise/adult-obesity
48. U.S Census Bureau's American Community Survey. https://data.census.gov/cedsci/table?q=age&g=0100000US.050000&y=2019&tid=ACSST5Y2019.S0101&hidePreview=true (2019).
49. 2020 US Presidential election County Level Election Results. https://github.com/tonmcg/US_County_Level_Election_Results_08-20
50. van der Walt, S., Colbert, S.C. & Varoquaux, G. The NUMPY array: a structure for efficient numerical computation. *Comput. Sci. Eng.* **13**, 22–30 (2011).
51. McKinney, W. Data structures for statistical computing in Python. In: van der Walt, S. & Millman, J., editors. *Proceedings of the 9th Python in Science Conference*. 51–6 (2010).
52. Alcántara, J., Chico, B., Simancas, J., Díaz, I. & Morcillo, M. Marine atmospheric corrosion of carbon steel: a review. *Materials* **10**(4), 406 (2017).
53. Scheuch, G. Breathing is enough: for the spread of influenza virus and SARS-CoV-2 by breathing only. *J. Aerosol. Med. Pulm. Drug. Deliv.* **33**(4), 230–234 (2020).
54. Hansson, G.C. Mucus and mucins in diseases of the intestinal and respiratory tracts. *J. Intern. Med.* **285**(5), 479–490 (2019).
55. Howard, J. *et al*. An evidence review of face masks against COVID-19. *Proc. Nati. Acad. Sci.* **118**(4), e2014564118 (2021). doi:10.1073/pnas.2014564118
56. George, L.C. *et al*. Inhaled salts reduce symptoms in mildly symptomatic COVID-19 patients in Bangalore (manuscript in review) (2021).
57. US Environmental Protection Agency's Air Quality System. https://www.epa.gov/air-trends/air-quality-cities-and-counties